Technical Report
University Of Wisconsin-Madison

(To be completed by RSP or the Department)

Project Title:	**Analysis of New Spectral Constraints on Jupiter's Cloud Structure**
Award Number:	**NNX09AE07G**
UW Account Number:	**PRJ23YA**
For the Period of:	**5/1/2012 through 4/30/2013**
Principal Investigator:	**Lawrence Sromovsky**
Date Submitted:	**2/21/2013**
Location:	**University of Wisconsin - Madison Space Science and Engineering Center 1225 West Dayton Street Madison, WI 53706**
Reports will be sent to:	**Max Bernstein Max.Bernstein@nasa.gov NSSC-Grant-Report@mail.nasa.gov**

SSEC Number (Internal) ***6453***

(To be completed by the Principal Investigator)

Inventions Report:

☒ No Inventions resulted from this award
☐ Yes

Inventory Report:

☒ No federally owned equipment is in the custody of the PI
☐ Yes

Publications: (Please list)

Peer Reviewed Publications:

Sromovsky, L.A., and P.M. Fry 2010. The source of 3-micron absorption in Jupiter's clouds: a reanalysis of ISO observations with new NH3 absorption models. *Icarus* **210**, 211-229.

Sromovsky, L.A., and P.M. Fry, 2010. The source of 3-micron absorption in Jupiter's clouds: constraints from 2000 VIMS observations. *Icarus* **210**, 230-257.

Sromovsky, L.A., and P.M. Fry, V. Boudon, A. Campargue, and A. Nikitin 2011. Near-IR methane absorption in outer planet atmospheres: comparison of line-by-line and band models. *Icarus* **218**, 1-23. (Partially supported by a Planetary Atmospheres Grant)

Li, Liming, K. H. Baines, M. A. Smith, R. A. West, S. Perez-Hoyos, H. J. Trammell, A. A. Simon Miller, B. J. Conrath, P. J. Gierasch, G. S. Orton, C. A. Nixon, G. Filacchione, **P. M. Fry**, and T. Momary. (2012), Emitted power of Jupiter based on Cassini CIRS and VIMS observations, J. Geophys. Res., 117, E11002.

Abstracts/Conference Presentations:

Sromovsky, L.A. and P.M. Fry. 2009. Evidence for widely distributed ammonia ice on Jupiter. *Bull. Am. Astron. Soc.* **41**, 1006.

Sromovsky, L.A. and P.M. Fry. 2010. Evidence for NH_4SH as the primary 3-micron absorber in Jupiter's Clouds. *Bull. Am. Astron. Soc.* **42**, 1010.

Sromovsky, L.A. and P. M. Fry. 2011. Comparison of line-by-line and band-model calculations of methane absorption in outer-planet atmospheres. Presented at the EPSC-DPS Joint Meeting in Nantes, France (43^{rd} DPS meeting).

Summary of Technical Effort: (Usually several paragraphs. Please feel free to attach additional pages if you wish.)

OBJECTIVES: We aimed to develop improved models of Jovian cloud structure using a combination of imaging and spectral observations acquired during the New Horizons 2007 flyby of Jupiter, and complementary data provided by Galileo and Cassini imaging and spectral observations acquired during the Cassini flyby of Jupiter at the end of 2000. The main New Horizons instrument of interest to this investigation is named Ralph, and includes a visible and near-IR multi-spectral imager (MVIC) and a near-IR Linear Etalon Imaging Spectral Array (LEISA). The latter is analogous to the Cassini VIMS and Galileo NIMS instrument but covers the 1.25-2.5 micron spectral range, compared to 0.3-5 microns for VIMS and 0.7-5.2 microns for the Galileo NIMS. LEISA's great advantage is the vastly better spatial resolution, with sub-spacecraft resolution ranging from 137 km/pixel at 32.44 RJ to 350 km at 82.3 RJ. VIMS best at Jupiter was 4900 km. Thus these data provide complementary spectral ranges, spatial coverages, and spatial resolutions. Variations in methane, ammonia, and collision-induced absorption with wavelength will be used to probe the vertical structure of clouds; we also plan to use high-resolution observations to infer vertical location from the ratio of spatial variations in cloud reflectivity at wavelengths with different penetration depths.

TASKS: (1) Image and Spectral Data Processing; (2) Characterization of spectral types, (3) Inversion of cloud structure from near-IR spectra, (4) Characterization of differences between New Horizons and Cassini Epochs, and (5) Combined analysis of CCD imagery and spectra.

PROGRESS DURING YEAR 4:

NOTE: *This is a progress report, instead of a final report, and is written under the assumption that a requested second no-cost extension will be granted.*

Work on processing eleven VIMS data sets to produce calibrated cubes with navigation backplanes was carried out in support of the above paper on Jupiter's total emitted power (Liming Li, prime author).

Analysis of CCD image data in combination with spectra (Task 5) is still in its initial stages, remaining at essentially the same state as described in last year's progress report.

The in-preparation paper on analysis of NICMOS observations of Jupiter has also not progressed, primarily because of uncertainties in how to handle potential absorption by NH_4SH and/or NH_3 particles in the F204M filter band, complicating the spatial modulation analysis, which is only simple if the aerosol properties can be assumed the same for both filter bands. As noted in last year's report, the spatial modulation technique applied to Cassini ISS images of Jupiter, using MT2 and CB2 filters resulted in unexpectedly high pressures, roughly twice the values expected from the near-IR analysis. This visible-near IR inconsistency in modulation pressure inferences is still not understood. We hoped that the New Horizons LEISA observations might provide a good data set for reaching that understanding. By selecting near-IR wavelengths that provide useful vertical sensitivity ranges but avoid potential particulate absorption features, we hope to make a clean comparison with the Cassini ISS CCD results.

Unfortunately, our progress has also been slow in making needed corrections to New Horizons LEISA spectral imaging observations that are needed to obtain calibrated spectra of discrete features, in part because we have not been able to apply sufficient effort to the task because of resource conflicts with other projects and with proposal and proposal review efforts. However, we did make considerable progress and now have reached a point at which corrected image cubes have been created. This has been a complicated correction. Recall that a full spectrum for the target region thus requires spatial scanning in the direction in which wavelength varies, taking image frames at each scan step. A monochromatic image can then be formed by assembling from top to bottom, line by line, the same wavelength row from each successive frame of the observation. The consequences of this are that each row of a monochromatic image has an effective acquisition time different from all other rows, and that different monochromatic images have different start times. This means that a specific cloud target can, and generally will, appear at different image locations at different wavelengths. This would be true even if the camera pointing did not vary during the image scan, which it does, and even if the cloud target stayed at the same latitude and longitude, which it does not.

The first step was to extract and process pointing information so that observations can be remapped to a latitude-longitude grid for each wavelength, with backplanes of time and viewing geometry. Since the wavelength varies slightly across a line in the raw image plane, we also had to interpolate in wavelength, that is to say in the y-direction in the raw image plane. We have produced prototype image cubes with dimensions of latitude (0.25 degree spacing), longitude (0.25 degree spacing), and wavelength (5 nm spacing). This remapping takes out the major factor that causes cloud features to appear at different image locations in different wavelengths. An additional refinement in the remapping would be to compensate for motion of features, due to Jupiter's zonal wind field. For individual dataset cubes this compensation is probably not necessary, though it would be required for any mosaicking of multiple cubes. In Figure 1 we show two bands of a remapped cube as a red/green image. In the blowup of the equatorial region, seen in the lower left window, there are dark features with longitudinal extents of around 0.5 degrees. With a per-image exposure time of 0.314 seconds, there is approximately 0.5 degrees of rotation of the planet between the acquisition of the lines of different wavelength. If the navigation and remapping of image lines widely separated in wavelength were not accurate, dark (or bright) features of that size would not remain coherent.

There are some dataset anomalies to be dealt with yet. One is the units of the calibrated datasets. Whereas the relevant project document (New Horizons SOC to Instrument Pipeline ICD) states that the units are radiance (with units W/cm^2/sr), the units appear to be spectral photon radiance (photons/micron/sr). We are currently communicating with the project data engineer to straighten this out. There are also some residual raw image bias or scattered light issues to deal with. Bias in the raw images manifest itself as vertical streaks in the processed monochromatic images. Where scans begin and end off the planet, blank bias images (that are subtracted from each raw image) can mostly rectify the problem. However, when the planet fills the entire scan (as is the case for several of the datasets), this correction cannot be applied.

In preparation for carrying out the proposed principal component analysis, we acquired the IDL-based software called ENVI, which is specifically designed to facilitate the analysis of hyperspectral data sets, like the one generated by LEISA. This has been installed, and utilities have been written to generate ENVI-compatible image headers, and the datasets can now be read by and manipulate by ENVI. We can thus use ENVI's PCA and classification tools to explore the datasets. Figure 1 shows an ENVI display of a LEISA cube with magnified section, along with an extracted spectrum.

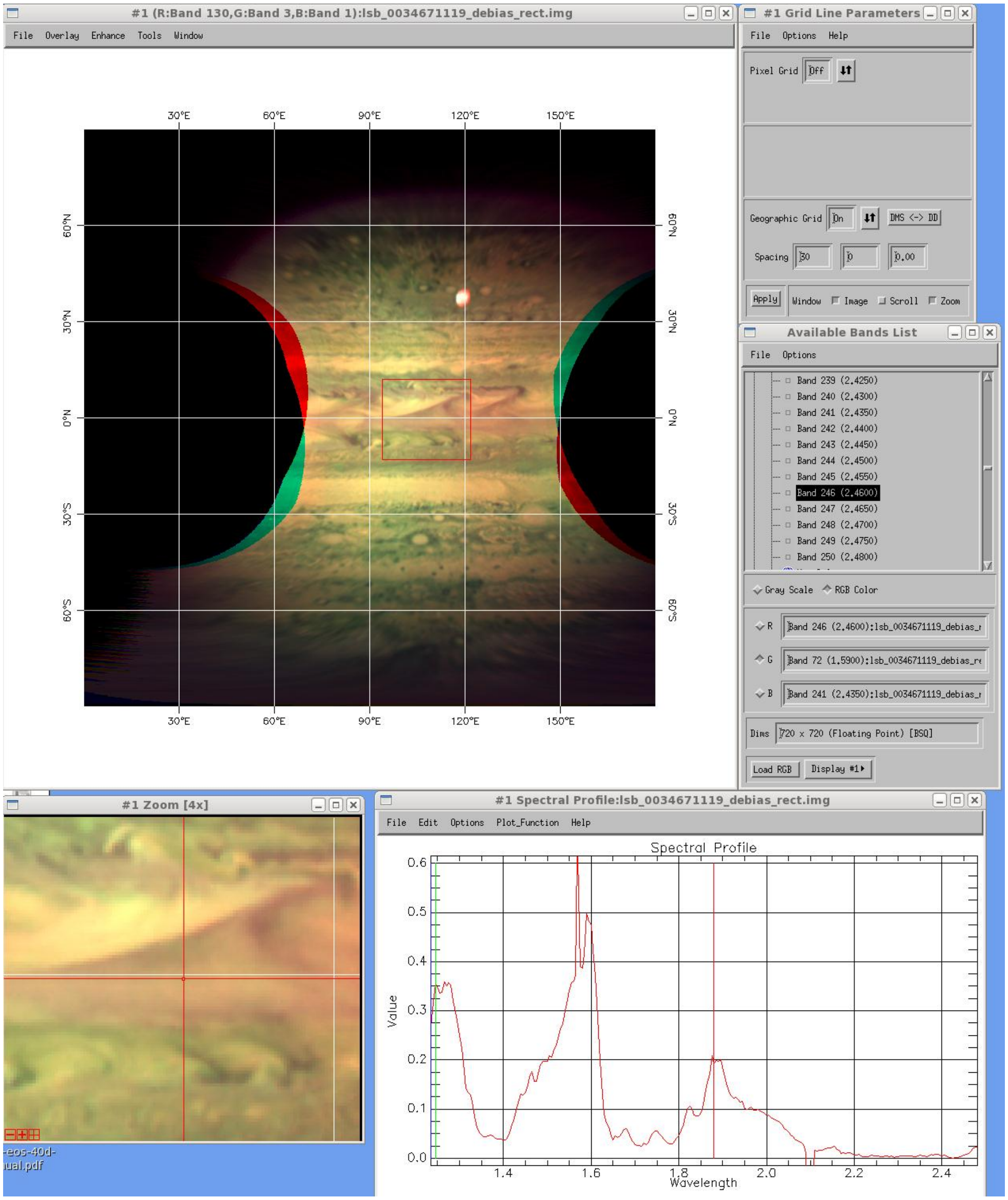

Figure 1. ENVI display comparing corrected and remapped LEISA images at two wavelengths to verify geometric alignment of wavelengths acquired at different times.

We have also begun the process of comparing LEISA observations with NICMOS and VIMS observations of Jupiter, to provide a sanity check on radiometric calibration and offset (or low light level) issues, as well as to begin the process of characterization of temporal changes between Cassini (2000) and New Horizon (2007) epochs (task 4). Images from all three data sets are shown in Figure 2. Although a precise comparison is prohibited by time differences between the data sets, we find general agreement on the I/F calibration that we have assumed (based on units of photon radiance) but, as illustrated in Figure 3, we find significant discrepancies in the regions of low I/F.

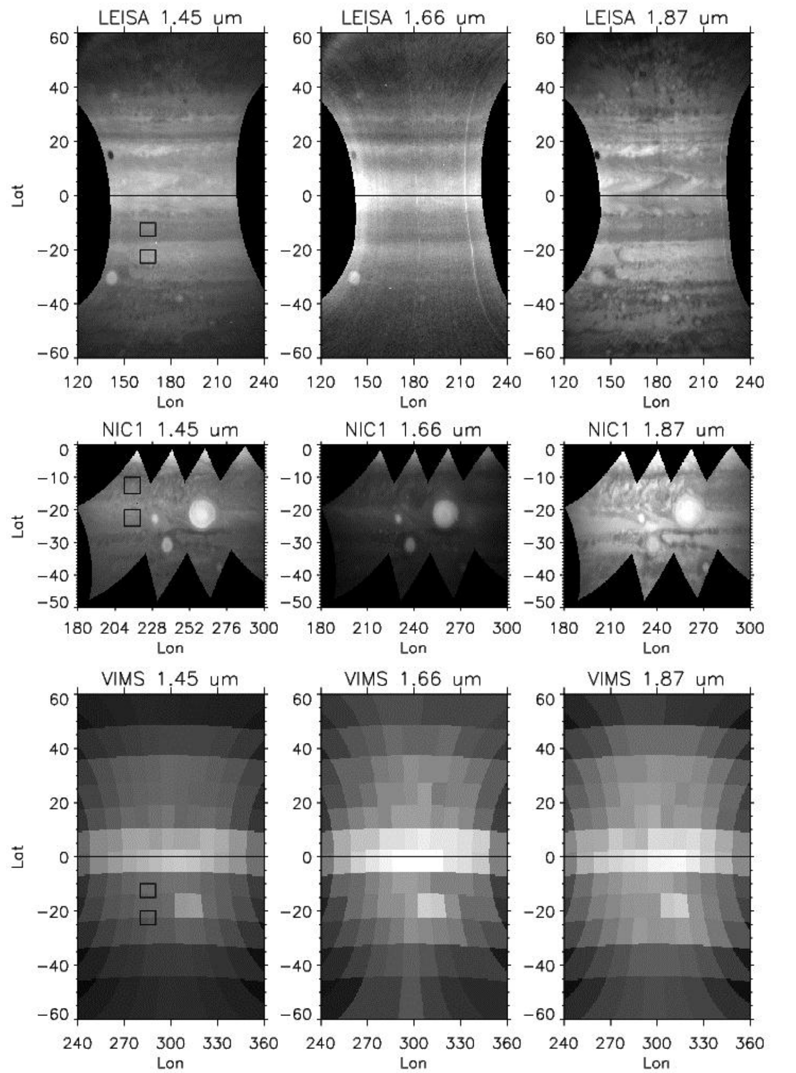

Figure 2. Comparison of remapped images of Jupiter from LEISA (February 2007), HST NICMOS (May 2008) and VIMS (December 2000). Spectral comparisons were made for SEB (10S-15S) and STZ (20S-25S) to avoid regions with significant temporal changes. Spectra were extracted from locations marked by black squares in Figure 3. Black to white corresponds to the I/F range of 0-0.18 for the 1.45-micron images, 0-0.05 for the 1.66-micron images, and 0-0.25 for the 1.87-micron images. The NICMOS images have bandwidths of 0.197, 0.017, and 0.0194 microns, from left to right.

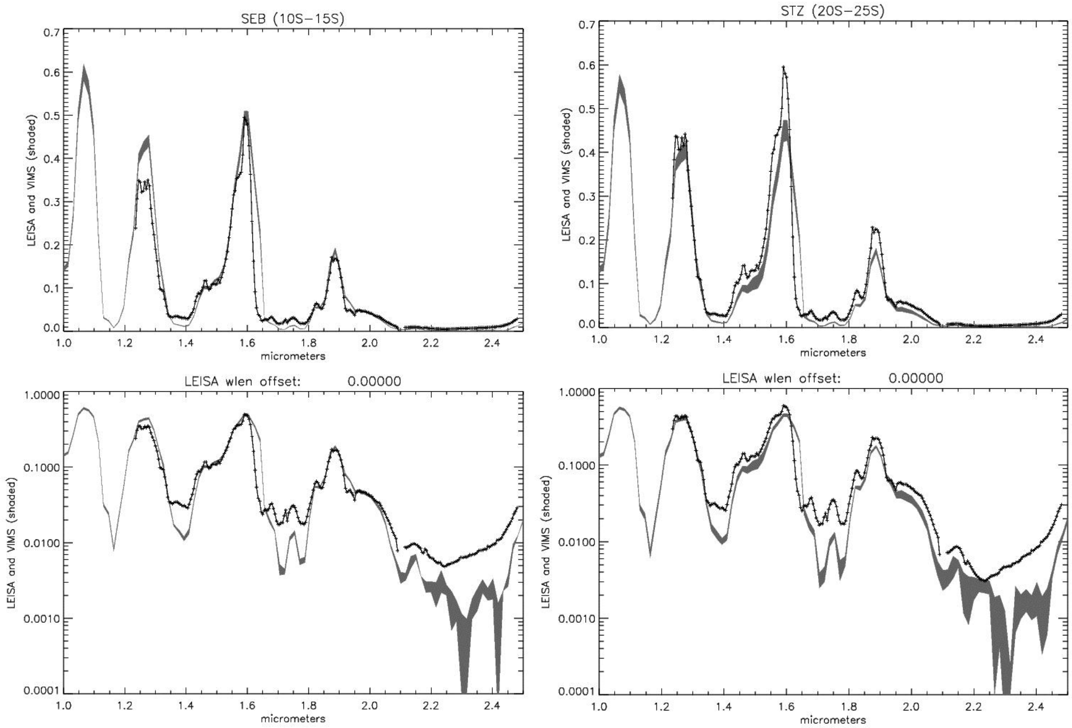

Figure 3. Left: Comparison of spectra fsrom LEISA (lines with points) and VIMS (shaded curve) in the region of the SEB (left) and STZ (right). Specific locations from which these spectra are extracted are identified by square boxes plotted in the left column of images in Figure 2. *The comparisons should be ignored in the 1.6-1.68 micron region where a joint in the VIMS order-sorting filter causes response anomalies.* These plots also illustrate a potential problem with low-I/F regions of the spectrum, although this might be due to temporal changes in high altitude haze amounts. These are the first detailed comparisons we know of between LEISA and VIMS atmospheric spectra.

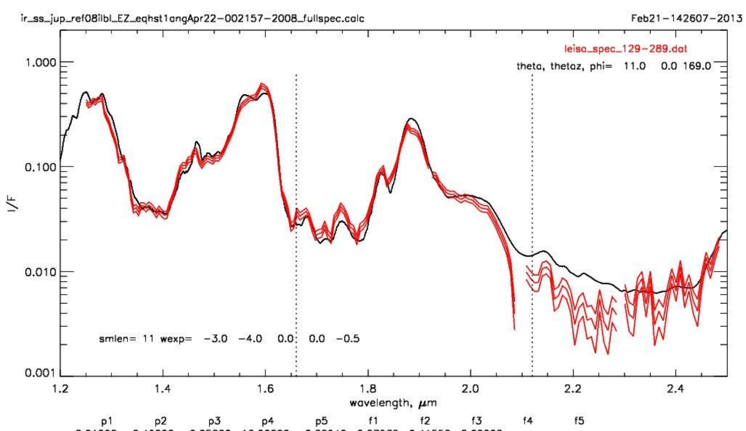

Figure 4. Comparison between LEISA spectrum (red) and model spectrum (black). This validates the LEISA wavelength calibration and demonstrates the compatibility of LEISA observations and radiative transfer modeling of Jupiter's spectrum.

For the comparison between LEISA observations and model calculations provided in Figure 4, we used a simple reflecting layer model, characterized by pressure, fractional coverage, and wavelength dependence exponent for each of two layers. In this case, the layers are located at 10 mb and 490 mb, with respective fractions of 0.079 and 0.416. The spectral details are well matched by the model in spite of its simplicity.

I/F value disagreements in Figure 3 between LEISA and VIMS spectra in the strongly absorbing regions might very well be due to temporal variations in haze optical depth. However, the NICMOS 1.66-micron image from 2008 is quite a bit darker (in Figure 2) than either VIMS or LEISA, suggesting that they may both be suffering from a low light level problem. Further analysis of such comparisons may be needed to settle this issue. A more meaningful comparison will be possible once LEISA spectral data cubes are integrated over appropriate bands with appropriate weighting to simulate the spectral weighting of the NICMOS band-pass filter images.

PLANS FOR NEXT YEAR:

Once the LEISA calibrations are verified, we can proceed to apply principal component analysis and spatial modulation analysis to the LEISA observations at multiple wavelengths and hopefully demonstrate a consistency between these near-IR observations and the Cassini ISS results at shorter (CCD) wavelengths. This should lead to a paper on results from both data sets. It remains unclear, however, whether we will be able to use these results to reach a satisfactory explanation for the NICMOS analysis, nor whether the remaining issues in the NICMOS paper in preparation can be sufficiently resolved to allow completion.

We will apply inversion techniques to determine cloud structure parameters, going beyond the pressure level of modulating layers and PC analysis, to infer optical depth, particle size, and to some degree, composition (Task 3). We will also adapt our automated fitting algorithm to handle the band-pass filter center-to-limb (CTL) observations and apply that to CTL results obtained from Cassini ISS images as described previously (Task 5).